Carbohydrate Research 343 (2008) 2463–2467

Contents lists available at ScienceDirect

Carbohydrate Research

journal homepage: www.elsevier.com/locate/carres

Note

In situ synthesis of amylose/single-walled carbon nanotubes supramolecular assembly

Liqun Yang *, Bifang Zhang, Yuting Liang, Bin Yang, Tao Kong, Li-Ming Zhang

Institute of Polymer Science, School of Chemistry and Chemical Engineering, Sun Yat-Sen University, PR China

ARTICLE INFO

Article history:
Received 30 October 2007
Received in revised form 31 March 2008
Accepted 13 June 2008
Available online 9 July 2008

Keywords:
Amylose
Single-walled carbon nanotubes
Supramolecular assembly
Vine-twining polymerization

ABSTRACT

A supramolecular assembly of amylose and single-walled carbon nanotubes (SWNTs) was synthesized in situ through vine-twining polymerization. Raman analysis indicated that the amylose–SWNTs supramolecular assembly was formed after the polymerization and SEM images displayed the twisted ribbons in the SWNTs wrapped by amylose. The dispersion stability of the SWNTs in aqueous solutions was improved by the wrapping of short-chain amylose molecules around the SWNTs.

Single-walled carbon nanotubes (SWNTs)[1] are single sheets of graphite rolled into seamless cylinders with a diameter of about 1 nm and a length of several micrometers, of which the surface and channel are nonpolar and hydrophobic. Since their discovery, SWNTs have been anticipated as a new potential material because of their excellent electrical and mechanical properties. However, the poor dispersion stability of SWNTs in solution has greatly limited their applications. Although covalent modification of the surface has helped to improve their dispersion stability, these modifications also destroy the chemical structure of the SWNTs and thus affect their physical properties.[1] To solve this problem, non-covalent modification of SWNTs by wrapping polymers around them was proposed.[2] Recently, wrapping amylose molecules around nanotubes has attracted much interest as a means for improving the dispersion stability of SWNTs in aqueous solutions.[1,3,4] Lu et al.[5] reported that helical amylose–SWNTs complexes showed good hydrophilicity and biocompatibility. This implies that the amylose–SWNTs complexes may open the application of SWNTs in the biomaterial field.

It is well known that amylose can be a host molecule for a helical complex when a guest molecule with a sufficiently long linear hydrophobic segment is available. In such a complex, the helical amylose is composed of six to eight glucose units per turn with a cavity diameter from 0.54 to 0.97 nm.[6] All of the hydroxyl groups of amylose are directed to the outside, and the channel of the helix is hydrophobic. Thus, the hydrophobic interaction is a driving force for the complex formation. Based on the similar sizes of SWNTs and the channel of helical amylose, amylose has a tendency to enwrap SWNTs through favorable hydrophobic interaction. Star et al.[1] first reported that the dispersion stability of SWNTs in aqueous solutions was improved by supramolecular assembly with helical amylose. The helical conformation of amylose was initially formed by complexation with iodine, and then subsequent treatment with SWNTs displaced the iodine molecules inside the helix. However, large steric hindrance exists in the complex formation between SWNTs and amylose, as shown in Scheme 1. Kim and Lu et al.[3,5] prepared soluble SWNTs by wrapping amylose around the nanotubes in aqueous dimethyl sulfoxide (DMSO), but the dispersion stability of SWNTs in pure water was still poor.

In this work, to reduce steric hindrance during the complexation process, and further improve the dispersion stability of SWNTs in aqueous solutions, amylose–SWNTs (Am–SWNTs) supramolecular assembly was done in situ through vine-twining polymerization (Scheme 2). The enzymatic polymerization for the synthesis of amylose occurred in the presence of SWNTs. Similar methods were recently reported to synthesize polymer inclusion complexes of amylose and hydrophobic compounds,[7–10] and amylose–lipid complexes.[11]

A homogeneous black aqueous solution was obtained after the enzymatic polymerization of amylose in the presence of SWNTs (Fig. 1A-a). The resulting solution was stable and exhibited no precipitation for 2–3 weeks. In contrast, agglomeration and precipitation occurred in pure aqueous solution of the SWNTs, even after ultrasonic dispersion (Fig. 1A-b). The dispersion stability of the SWNTs was assessed by UV–vis spectrophotometric analysis. The profiles of the absorption spectra in Figure 1B were similar to those of the reported SWNTs and amylose complex, which was formed in

* Corresponding author. Tel.: +86 20 84110934; fax: +86 20 84112245.
E-mail address: yanglq@mail.sysu.edu.cn (L. Yang).

0008-6215/$ - see front matter © 2008 Elsevier Ltd. All rights reserved.
doi:10.1016/j.carres.2008.06.031

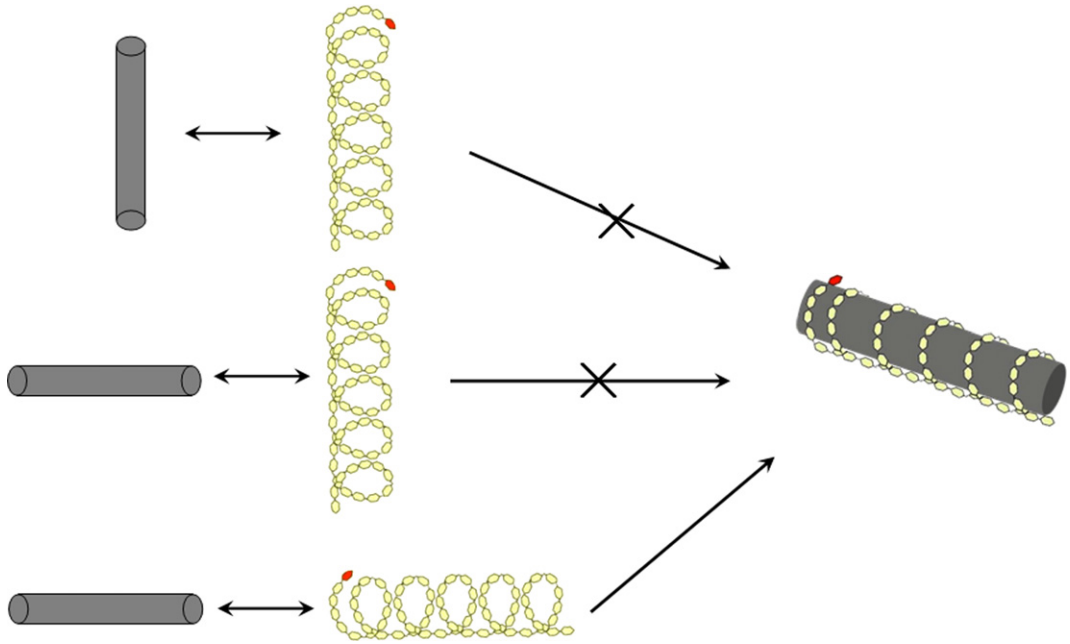

Scheme 1. Presentation of steric hindrance of SWNTs entering helical amylose.

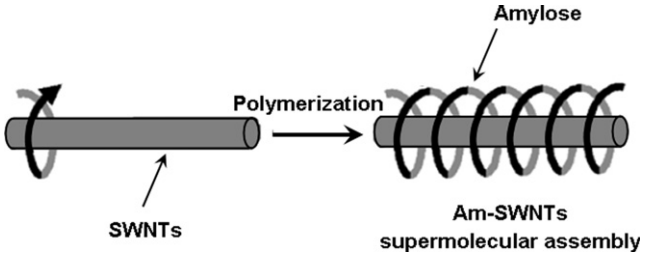

Scheme 2. In situ synthesis of the Am–SWNTs supramolecular assembly through vine-twining polymerization.

aqueous DMSO.[3] The absorbance of the Am–SWNTs black solution was higher than that of the pure SWNTs solution (Fig. 1B), indicating that the dispersion stability of SWNTs was improved after the enzymatic polymerization.

Figure 2 shows SEM images of the pure SWNTs and the Am–SWNTs. The pure SWNTs were found to be entangled and even agglomerated in aqueous solution (Fig. 2a). After the enzymatic polymerization, the SWNTs became separated individual bundles (Fig. 2b), and displayed loosely twisted ribbons on the nanotubes (Fig. 2c). This twisted structure was similar to the reported SWNTs–amylose complexes prepared in aqueous DMSO solutions.[3] This implies that an amylose–SWNTs supramolecular assembly was formed, in which amylose encapsulated SWNTs as a guest molecule.

Raman scattering is a more powerful technique to probe the structure and property relationships of both SWNTs and their supramolecular assemblies.[5] The Raman spectra of Am–SWNTs, pure SWNTs, and amylose are shown in Figure 3. It can be clearly seen that for the pure SWNTs sample the radical breathing modes (RBMs) are positioned at 163, 167, 202, 232, and 262 cm^{-1} (curve (b) of Fig. 3B). According to the inversely proportional relationship between RBM (ω_{RBM}) and the SWNTs diameter (d): $d = 224/(\omega_{RBM} - 14)$,[12] the observed peaks correspond to SWNTs with diameters of 1.5, 1.4, 1.2, 1.0, and 0.90 nm. The dominated RBM at 262 cm^{-1} up-shifts to 267 cm^{-1} in the spectrum of Am–SWNTs

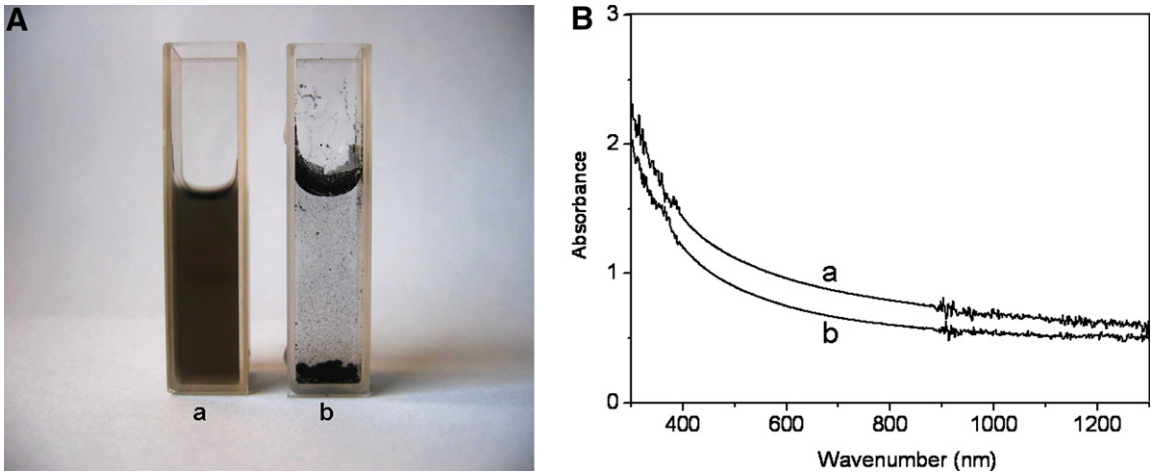

Figure 1. Photograph (A) and UV–vis spectra (B) of (a) Am–SWNTs and (b) pure SWNTs in aqueous solutions.

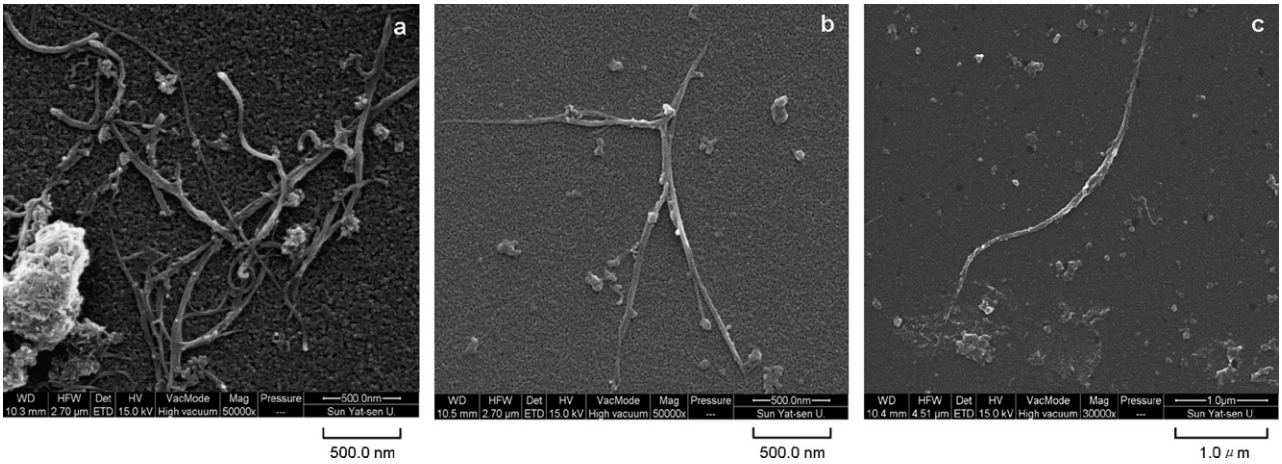

Figure 2. SEM images of (a) the pure SWNTs, (b) and (c) Am–SWNTs.

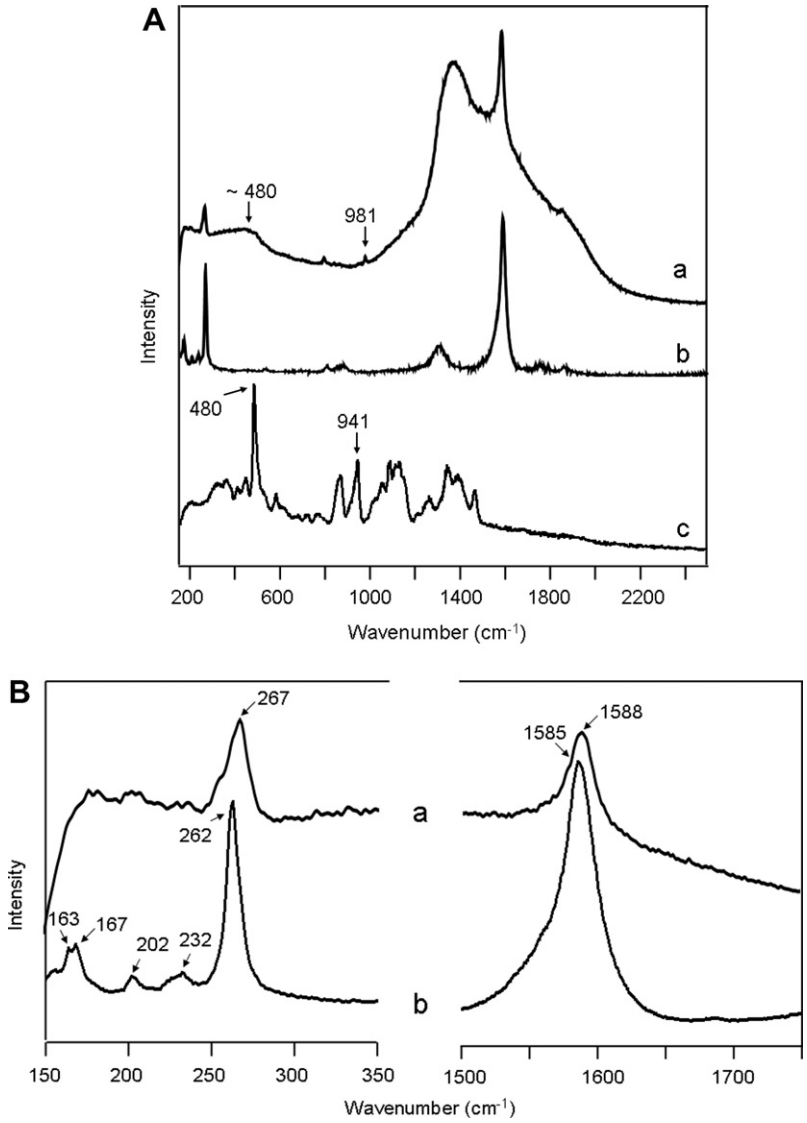

Figure 3. Raman spectra of (a) Am–SWNTs, (b) the pure SWNTs, and (c) amylose (B is partly enlarged from A).

(curve (a) of Fig. 3B). As the RBM band is sensitive to the diameter and the interactions of SWNTs, a shift of 5 cm^{-1} indicates a debundling process for the surface modification of SWNTs ropes.[13] In addition, a strong band located at 1585 cm^{-1} in the spectrum of the pure SWNTs is assigned to the graphite band (G-band) arising from sp^2-hybridised carbon atoms on the wall of SWNTs.[14] And

about 3 cm^{-1} shift in the G-band can be observed in the spectrum of Am–SWNTs. The shifts in the positions of both the RBM and G-band are probably caused as a result of non-covalent interactions between amylose and SWNTs as described earlier.[5,13]

In the Raman spectrum of amylose (curve (c) in Fig. 3A), the band at 480 cm^{-1} is attributed to skeletal modes of pyranose rings of amylose,[15,16] which becomes broad in the spectrum of Am–SWNTs in curve (a). The peak at 941 cm^{-1} is due to α-(1→4)-glycosidic stretching modes of amylose in curve (c).[16] This stretch shifts to 981 cm^{-1} in the Raman spectrum of Am–AWNTs. This result is in agreement with the Raman analysis of complexes of SWNTs and potato amylose,[6] indicating that the debundling of SWNTs is through the wrapping of helical amylose molecules around the SWNTs. It further proves that the amylose–SWNTs supramolecular assembly has been formed after the enzymatic polymerization.

The amylose–SWNTs supramolecular assembly was synthesized through the vine-twining polymerization, that is, the polymerization of amylose occurred in the presence of SWNTs. As shown in Scheme 3a, the polymerization[17] is initiated from a primer of maltoheptaose and proceeds from α-D-glucose 1-phosphate (Glc-1-P) as a monomer catalyzed by phosphorylase, where a glucose residue was transferred from Glc-1-P to the non-reducing terminus of α-glucan chain, releasing inorganic phosphate (HPO_4^{2-}, Pi). This process is similar to active anionic polymerization. Therefore, the degree of polymerization (DP) of amylose, defined as the number of glucose units, could be controlled. By assuming that all the maltohexaose moieties were used as primers, the DP of amylose was approximated by phosphate analysis from

$$DP = (7 + N_{Pi}/N_{Glc7}) \quad (1)$$

where 7 is the number of glucose units of maltohexaose, N_{Pi}/N_{Glc7} is the molar ratio of the released inorganic phosphate and used maltohexaose, and N_{Pi} is determined from phosphate analysis.

The DP of amylose was estimated to be about 47 in this work. Thus, the structure of the Am–SWNTs supramolecular assembly is speculated to be that shown in Scheme 3b. This consists of long SWNTs entangled with hydrophilic helical amylose molecules. Such supramolecular structures have the advantage of not only

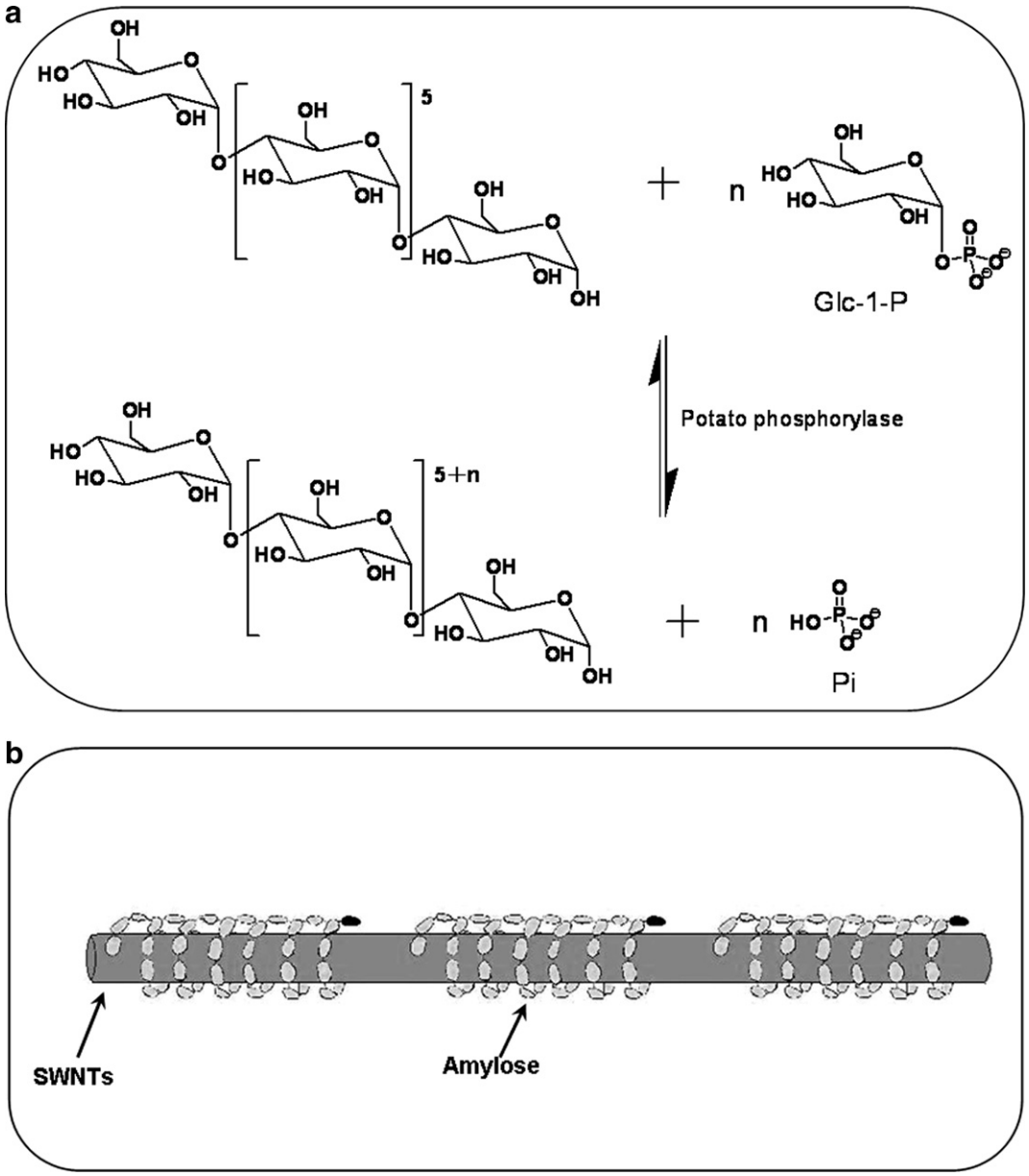

Scheme 3. (a) Synthesis of amylose by enzymatic polymerization. (b) The speculated supramolecular structure of Am–SWNTs.

reducing van der Waals interactions between SWNTs, but also increasing the hydrophilic property of SWNTs by the entangled amylose. As a result, the dispersion stability of SWNTs in aqueous solution was improved without the distinct agglomeration and precipitation. The good dispersion stability of SWNTs in aqueous solutions is also due to the lower DP of amylose, because the solubility of amylose in aqueous solution has a sharp minimum at DP of about 80; shorter (DP <50) and longer molecules (DP >2000) are much more soluble.[18,19]

In conclusion, the major finding of this work is that the dispersion stability of SWNTs in aqueous solutions could be improved through the vine-twining polymerization. Raman analysis and the SEM images proved that the amylose–SWNTs supramolecular assembly was formed after the polymerization. Further experiments are in progress and the results will be described in detail in future publications.

1. Experimental

1.1. Materials

Maltoheptaose was bought from the Supelcov Company, USA; Glc-1-P was purchased from Acros. SWNTs with diameters of less than 2.0 nm and length of 5–15 μm were bought from Shenzhen Nanotechnologies Co. Ltd, China. Amylose was purchased from Sigma Aldrich.

Potato phosphorylase was isolated according to previously published work.[20] Briefly, washed, peeled and sliced potatoes (2 kg) were liquidized in a juice extractor. The crude extract was added to a sodium sulfite solution and centrifuged at 5 °C. The supernatant was heated at 55–56 °C for 45 min to destroy α-amylase activity and then centrifuged. The density of the resulting supernatant was adjusted to 1.09–1.15 by slowly adding ammonium sulfate and was kept at 5 °C overnight. After centrifugation, the precipitates containing phosphorylase were dissolved in Tris buffer (pH 7.2) and were stored at 5 °C until use in amylose synthesis. As one molecule of phosphate is produced for each glucose molecule attached to amylose chain, phosphate analysis was used to determine the phosphorylase activity.[21]

1.2. Synthesis of Am–SWNTs supramolecular assembly

SWNTs (5 mg) were added to 15 mL of sodium citrate buffer (pH 6.2) and were dispersed by ultrasonication for 45 min. Then, 10 mL of phosphorylase solution, 0.7 g of Glc-1-P, and 50 mg of maltoheptaose were added, and the reaction was carried out by stirring and discontinuous ultrasonication at 37 °C for 3 h. The resulting black supernatant containing SWNTs was separated after the reaction solution was kept at 5 °C overnight. The DP of synthesized amylose was approximated by phosphate analysis.[8]

1.3. Characterization

UV–vis spectra were acquired using a UV–vis–NIR Spectrometer (UV-3150, Shimadzu, Japan). Scanning electron microscopy (SEM) observation was carried out on a field emission scanning electron microscope (JSM-6330F, JEOL Ltd, Japan). Raman scattering studies were performed with a Laser Micro-Raman Spectrometer (Renishaw inVia, Britain) at 1 cm^{-1} resolution, using a laser excitation wavelength at 785 nm with 300 mW. An aqueous sample of Am–SWNT was filled in a glass capillary tube and then was measured. The band of the glass capillary tube was located at about 1380 cm^{-1}. Other solid samples were measured on a clean glass microscope slide.

Acknowledgments

This work was supported by the National Natural Science Foundation of China (20574089, 20676155) and the Scientific Research Foundation for the Returned Overseas Chinese Scholars from the State Education Ministry.

References

1. Star, A.; Steuerman, D. W.; Health, J. R.; Stoddart, J. F. *Angew. Chem., Int. Ed.* **2002**, *41*, 2508–2512.
2. Tasis, D.; Tagmatarchis, N.; Bianco, A.; Prato, M. *Chem. Rev.* **2006**, *106*, 1105–1136.
3. Kim, O. K.; Je, J.; Baldwin, J. W.; Kooi, S.; Pehrsson, P. E.; Buckley, L. J. *J. Am. Chem. Soc.* **2003**, *125*, 4426–4427.
4. Bonnet, P.; Albertini, D.; Bizot, H.; Bernard, A.; Chauvet, O. *Compos. Sci. Technol.* **2007**, *67*, 817–821.
5. Fu, C.; Meng, L.; Lu, Q.; Zhang, X.; Gao, C. *Macromol. Rapid Commun.* **2007**, *28*, 2180–2184.
6. Lii, C.; Stobinski, L.; Tomasik, P.; Liao, C. *Carbohydr. Polym.* **2003**, *51*, 93–98.
7. Kaneko, Y.; Kadokawa, J. *Chem. Rec.* **2005**, *5*, 36–46.
8. Kadokawa, J.; Kaneko, Y.; Nagase, S.; Takahashi, T.; Tagaya, H. *Chem. Eur. J.* **2002**, *8*, 3321–3326.
9. Kadokawa, J.; Nakaya, A.; Kaneko, Y.; Tagaya, H. *Macromol. Chem. Phys.* **2003**, *204*, 1451–1457.
10. Kadokawa, J.; Kaneko, Y.; Nakaya, A.; Tagaya, H. *Macromolecules* **2001**, *34*, 6536–6538.
11. Gelders, G. G.; Goesaert, H.; Delcour, J. A. *Biomacromolecules* **2005**, *6*, 2622–2629.
12. Rao, A. M.; Chen, J.; Richter, E.; Schlecht, U.; Eklund, P. C.; Haddon, R. C.; Venkateswaran, U. D.; Kwon, Y. K.; Tomanek, D. *Phys. Rev. Lett.* **2001**, *86*, 3895–3898.
13. Chambers, G.; Carroll, C.; Farrell, G. F.; Dalton, A. B.; McNamara, M.; Panhuis, M.; Byrne, H. J. *Nano Lett.* **2003**, *3*, 843–846.
14. Sanchez-Pomales, G.; Santiago-Rodríguez, L.; Rivera-Velez, N. E.; Cabrera, C. R. *Phys. Stat. Sol. A* **2007**, *204*, 1791–1796.
15. Fechner, P. M.; Wartewig, S.; Kleinebudde, P.; Neubert, R. H. H. *Carbohyr. Res.* **2005**, *340*, 2563–2568.
16. Schuster, K. C.; Ehmoser, H.; Gapes, J. R.; Lendl, B. *Vib. Spectrosc.* **2000**, *22*, 181–190.
17. Ziegast, G.; Pfannemuller, B. *Carbohydr. Res.* **1987**, *160*, 185–204.
18. Pfannemuller, B.; Mayerhofer, H.; Schulz, R. C. *Biopolymers* **1971**, *10*, 243–261.
19. Gidley, M. J.; Bulpin, P. V. *Macromolecules* **1989**, *22*, 341–346.
20. Roger, P.; Axelos, M. A. V.; Colonna, P. *Macromolecules* **2000**, *33*, 2446–2455.
21. Lowry, O. H.; Lopez, J. A. . *J. Bio. Chem.* **1946**, *162*, 421–428.